RAPID COMMUNICATIONS

PHYSICAL REVIEW C VOLUME 52, NUMBER 3 SEPTEMBER 1995

Evidence for a proton halo in ^{8}B: Enhanced total reaction cross sections at 20 to 60 MeV/nucleon

R. E. Warner,[1,2] J. H. Kelley,[3] P. Zecher,[3] F. D. Becchetti,[2] J. A. Brown,[3] C. L. Carpenter,[1,*] A. Galonsky,[3] J. Kruse,[3] A. Muthukrishnan,[1,†] A. Nadasen,[4] R. M. Ronningen,[3] P. Schwandt,[5] B. M. Sherrill,[3] J. Wang,[3] and J. S. Winfield[3,‡]

[1]*Oberlin College, Oberlin, Ohio 44074*

[2]*University of Michigan, Ann Arbor, Michigan 48109*

[3]*National Superconducting Cyclotron Laboratory, East Lansing, Michigan 48824*

[4]*University of Michigan, Dearborn, Michigan 48128*

[5]*Indiana University Cyclotron Facility, Bloomington, Indiana 47405*

(Received 1 May 1995)

Total reaction cross sections σ_R for ^{8}B, ^{12}C, and ^{14}N on ^{nat}Si were measured from about 20 to 60 MeV/nucleon. The σ_R for ^{12}C and ^{14}N compared reasonably well with conventional strong absorption and microscopic calculations. Measured σ_R for ^{8}B were slightly larger than those for the two heavier nuclei, and notably larger than the conventional calculations. The ^{8}B data were well reproduced by microscopic calculations using the same matter distribution used to explain the ^{8}B quadrupole moment data, and therefore provide new evidence for the existence of a proton halo in ^{8}B.

PACS number(s): 21.10.Gv, 24.10.−i, 25.60.+v, 27.20.+n

The existence of neutron-halo nuclei such as ^{6}He and ^{11}Li [1], discovered through measurements of their interaction cross sections σ_I, is one of the most exciting recent nuclear physics discoveries. Perhaps the best candidate [2] for a proton-halo nucleus is ^{8}B, whose last proton is bound by only 137 keV. Experimental evidence for a halo comes from both the large ^{8}B quadrupole moment [3] and recent measurements [4] of fragmentation into ^{7}Be+p, which show a longitudinal momentum distribution with a FWHM 3 times smaller than that predicted by Goldhaber theory [5] and observed for one-proton removal from other light projectiles. There is, however, controversy over whether the quadrupole moment requires a halo interpretation [2] or simply results from $E2$ core polarization [6].

Measurements [7] of σ_I at 790 MeV/nucleon indicated that ^{8}B has normal size, and there are claims [2,3] that cross-section measurements are insensitive probes for proton halos. This is untrue at lower bombarding energies, as we show in this paper; moreover we present σ_R measurements for ^{8}B+Si at 20–60 MeV/nucleon which strongly indicate a halo structure.

Our σ_R measurements require magnetic analysis and particle identification (PID) to obtain a narrow monoenergetic projectile beam which is stopped in one or more Si or CsI detectors [8]; reactions are then identified through pulse height analysis. Natural Si, contained in detectors, is a useful target since model calculations [9] predict σ_R's for most projectiles which differ by less than 0.5% for ^{28}Si and ^{nat}Si. In this experiment, a beam of ^{8}B was produced by fragmentation of 80 MeV/nucleon ^{18}O projectiles on a 0.5 mg/cm^2 ^{9}Be target, and passed though the A1200 analyzing system [10] at the National Superconducting Cyclotron Laboratory. Measurements also were made for ^{12}C and ^{14}N produced on a 0.6 mg/cm^2 C target. These secondary beams were delivered to the Reaction Product Mass Separator [11], which refines the velocity and momentum selection of fragments transmitted through the A1200 system.

The detector stack (see Fig. 1) included a plastic scintillator which measured time of flight (TOF), two parallel-plate avalanche counters (PPAC's) which selected projectiles sufficiently close to the detector axis, and 10 Si transmission detectors of alternating 100 μm (or 150 μm) and 1 mm thicknesses. A tight PID gate on TOF vs energy loss ΔE in the first thin Si detector selected the desired ion species.

The use of multiple Si detectors permitted simultaneous measurement of σ_R for several different energy ranges. Expected energy losses due to ionization in each detector were found by applying the scaling law $(dE/dx)=Z^2f(v)$ to an α-particle energy-loss table [12]; this permitted both detector calibration and reaction identification. Figure 2, showing ΔE in the first thick Si detector vs total energy loss in the

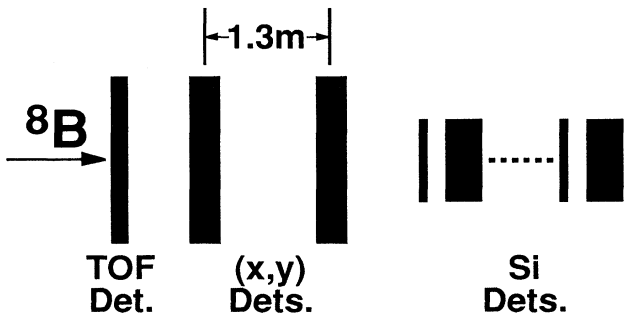

FIG. 1. Detector layout for measuring σ_R of ^{8}B, ^{12}C, and ^{14}N in Si.

*Present address: Phillips Exeter Academy, Exeter, NH 03833.

†Present address: University of Rochester, Rochester, NY 14627.

‡Present address: Institut de Physique Nucleaire, IN2P3-CNRS, 91406 Orsay Cedex, France.

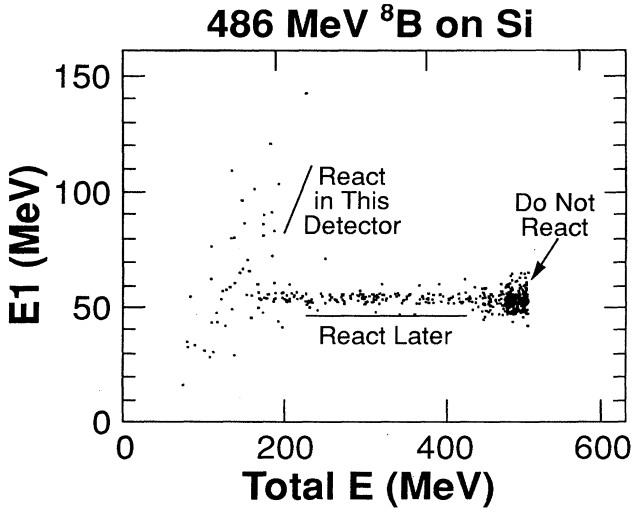

FIG. 2. Two-dimensional spectrum for 61 MeV/nucleon ^{8}B in Si: ΔE for second detector in Si stack vs energy deposited in entire stack.

entire telescope, qualitatively illustrates the occurrence of reaction events in different detectors; hence, in different energy ranges. By examining spectra such as Fig. 2, tight ΔE gates were set for each detector, to identify ions which had not yet reacted in that or preceding detectors. This analysis identifies not only high-Q reactions but low-Q fragmentation reactions, such as $^8\mathrm{B}\rightarrow{}^7\mathrm{Be}+p$, whose reaction products have smaller (dE/dx) than ^{8}B.

Data were analyzed for detectors grouped in pairs: a thick counter followed by a thin one. The probability η_n for a reaction to occur in the nth thick counter or any subsequent one was found from a single-dimensional total energy loss spectrum, such as Fig. 3, which was gated on PID, PPAC's and normal ΔE's for all preceding detectors. Likewise, the probability η_{n+1} was determined for the $(n+1)$st thick detector and succeeding ones.

Finally, from the difference $\eta_n - \eta_{n+1}$, we determined [8] σ_R for the energy interval determined by the nth thick detector and the following thin detector; these σ_R's are presented in Fig. 4. The ^{8}B cross sections are seen to be at least as large as those for the heavier projectiles. The horizontal "error bars" simply indicate the spread of energies at which reactions may occur in each detector pair; the uncertainty in these energies is considered to be only about 1% since stopping powers and ranges given by the available tables [12,13] agree to this accuracy. The principal systematic error in σ_R is thought to result from extrapolating to find the yield of low-Q reactions under the peak [8]; different extrapolating procedures agreed to within $\pm 4\%$, and the vertical error bars were obtained by adding this amount in quadrature to the counting statistical uncertainties.

Figure 4 also presents various model predictions. Two strong absorption (SA) model [9,14] calculations adequately predict the magnitude of σ_R for ^{12}C and ^{14}N, though not the ^{14}N energy dependence. Microscopic model [15,16] calculations fit the ^{12}C and ^{14}N data equally well. These employ harmonic oscillator (HO) matter density distributions for the projectiles and 3-parameter-Fermi densities for ^{28}Si—all obtained from electron scattering data [17]—and the Charagi-Gupta [18] parametrization of the nucleon-nucleon cross sections.

The three conventional calculations for ^{8}B generally underpredict the measured σ_R's by about 300 mb and, as

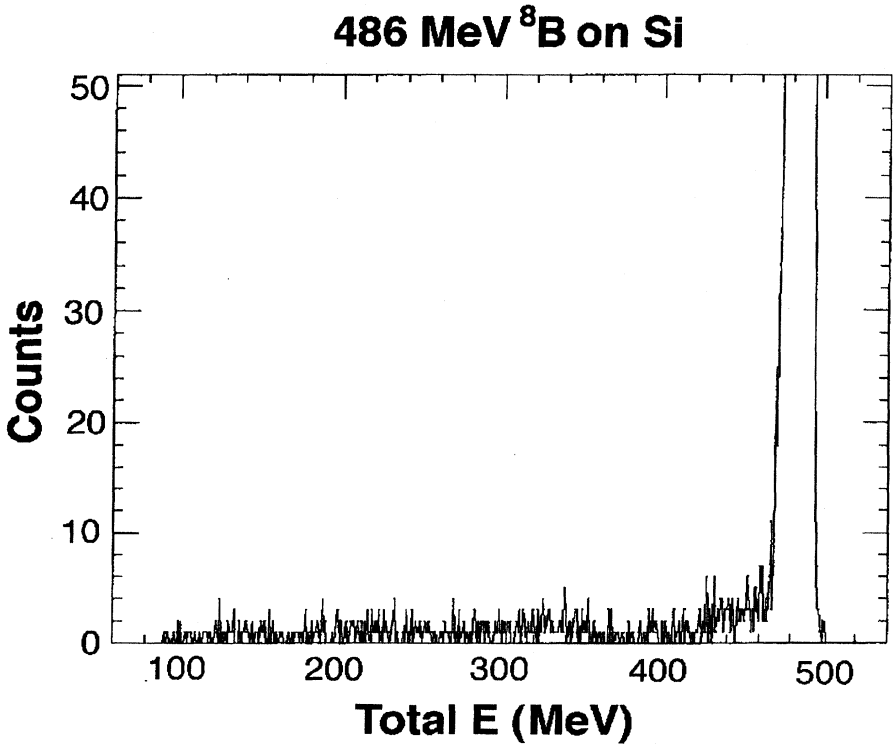

FIG. 3. Total energy recorded by 486 MeV ^{8}B projectiles in telescope after giving normal TOF, PPAC, and ΔE_1 signals.

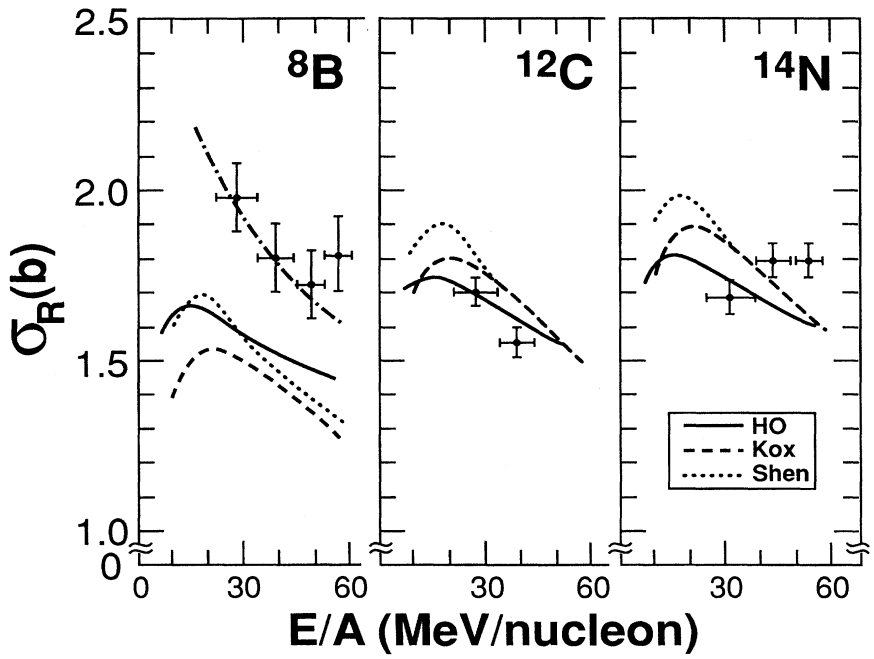

FIG. 4. σ_R vs E for ^{8}B, ^{12}C, and ^{14}N in Si. Dashed lines show SA model predictions; the solid lines show microscopic model predictions for harmonic oscillator projectile matter distributions; the dot-dash line shows the microscopic prediction for the ^{8}B matter distribution from Ref. [3].

expected, are lower than those for ^{12}C and ^{14}N. The discrepancy of the data with the microscopic calculation, which used a ^{9}Be HO form factor, is particularly significant since its rms matter radius of 2.52 fm exceeds that obtained elsewhere [2], for ^{8}B (2.26 fm) using HO wave functions.

We therefore repeated the microscopic calculations with the ^{8}B matter density distribution used in Ref. [3] to fit the quadrupole moment data; an excellent fit (dot-dash curve in Fig. 4) was obtained. This distribution has rms radii of 2.20 fm and 2.98 fm for the neutrons and protons, respectively. That for the whole nucleus is 2.72 fm, in close agreement with that obtained in Ref. [2] using Woods-Saxon wave functions.

We investigated [19] the possible contribution to the observed cross section by electromagnetic dissociation (EMD) of ^{8}B into ^{7}Be+p by the Si target. The virtual photon spectrum was found as in Ref. [20], and the photodissociation cross section was obtained by applying detailed balance to the reported [21] 0–10 MeV proton capture cross sections. $E1$ photons below 10 MeV were found to cause a 5 mb EMD cross section and exhaust 12% of the $E1$ photoabsorption sum rule [22]. Assuming that the remaining 88% goes into ^{7}Be+p at higher energies, or into such final states as ^{6}Be+d or ^{6}Li+2p, would add little to the 5 mb. Thus the total EMD cross section appears negligible compared with the 300 mb difference between our observed ^{8}B σ_R and the

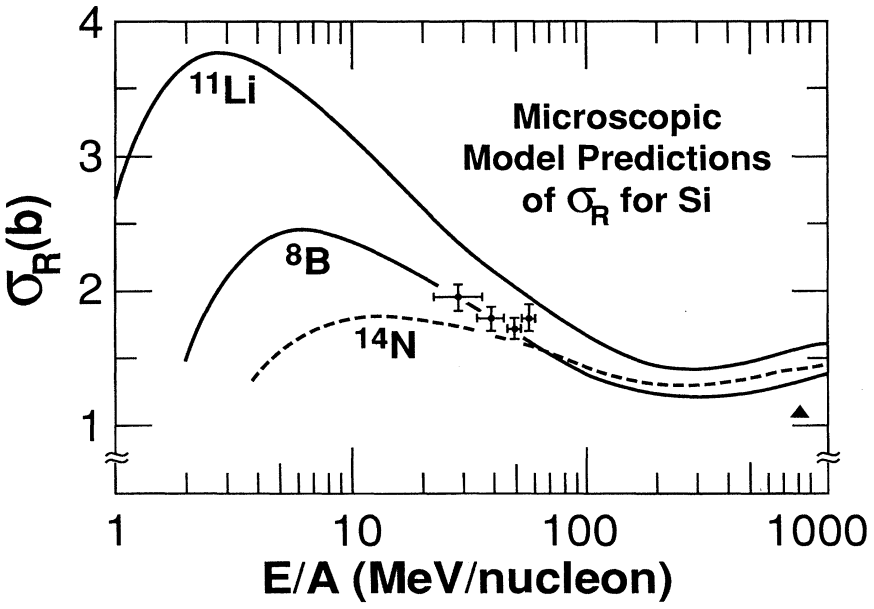

FIG. 5. Microscopic model predictions of energy dependence of σ_R for three projectiles on Si. Matter distributions [3,23] with halo components are used for ^{8}B and ^{11}Li. Crosses show our measurements for ^{8}B+Si, and the triangle shows an earlier measurement [7] for ^{8}B+Al.

conventional predictions; we therefore attribute the excess to nuclear effects.

Much lower interaction cross sections σ_I are observed for ^{8}B at 790 MeV/nucleon [7]. The difference must arise mainly from the increased transparency of nuclei at high energies. This is explained naturally by the microscopic model, which attributes σ_R to the sum of collisions between individual nucleon-nucleon pairs in the interacting nuclei. The ^{8}B halo, whose density at $r=10$ fm is only $\sim 10^{-4}$ of central density [3], plays a more important role at low energies where the increased average nucleon-nucleon cross section leads to collisions even in low-density regions. For example, the average σ_{NN} is 30 times larger at 5 MeV/nucleon, where the maximum σ_R is predicted, than at 790 MeV/nucleon. Figure 5 shows the energy dependence of microscopic σ_R predictions for ^{28}Si; matter densities for ^{8}B and ^{14}N were those previously referenced, and that for ^{11}Li was taken from Ref. [23]. Evidently, even though Coulomb repulsion eventually suppresses σ_R, at energies of a few MeV/nucleon the closest-approach distance is still small enough to allow collisions in the tails of the halo nuclei. The low-energy enhancement for ^{11}Li is especially pronounced.

We have calculated microscopic ^{8}B σ_R's at 790 MeV/nucleon for the three targets listed in Ref. [7]. All are about 25% larger than the measurements, one of which (^{8}B+^{27}Al) is shown (as a triangle) in Fig. 5. (Calculations using both SA [9] and microscopic models indicate no more than 1% difference between ^{27}Al and ^{28}Si targets.) In general σ_R is greater than σ_I since the former includes all reactions, and the latter excludes both inelastic scattering and target breakup with the projectile left intact. However, for such a loosely bound projectile as ^{8}B, one might not expect a large difference.

The quadrupole moment [3], fragmentation [4,24], and present σ_R data together make a strong case for the existence of a proton halo in ^{8}B, which is of interest not only in its own right but because the structure of ^{8}B is relevant to the solar neutrino problem [25]. More σ_R measurements would be useful at higher energies, where interaction cross-section σ_I measurements [7] do not indicate a halo; a microscopic model for calculating σ_I would be equally useful. Measurements at very low energies, where the microscopic model predicts maximum enhancement, are of special interest though difficult. Such an enhancement has already been reported [26] for the σ_R of an isomeric nucleus [^{18}F*, $\tau=234$ ns] with Si.

Note added in proof. After our paper was submitted, Pecina *et al.* [27] reported measurements of quasielastic (elastic plus slightly inelastic) scattering of ^{8}B and ^{7}Be on ^{12}C at 40 MeV/nucleon. By fitting their data with a semimicroscopic double folding model and coupled channels calculation, they deduced σ_R's for ^{8}B and ^{7}Be which differ only slightly and therefore do not support the existence of a substantial proton halo in ^{8}B. They also find smaller differences in rms radii of the proton and neutron distributions than those deduced from the ^{8}B quadrupole moment [3]. Since optical model analyses of elastic scattering do not always reliably predict σ_R [28] we believe it is important that the calculations of Pecina *et al.* [27] be tested against direct measurements of σ_R. More measurements of σ_R of ^{8}B on different targets, particularly at these energies, would be helpful in finally settling the ^{8}B halo question.

We thank Prof. Sam Austin for encouraging our measurements, and Dr. H. Kitagawa and Dr. I. Tanihata for sending us their ^{8}B and ^{11}Li matter distributions. We thank the staff of the NSCL for providing excellent beams, and especially D. Swan for assistance with detectors and Wen-Chien Hsi for help with computing. The work was supported by the National Science Foundation under Grants Nos. PHY-9122067, PHY-9208468, PHY-9214992, PHY-9312428, and PHY-9314783.

[1] I. Tanihata, H. Hamagaki, O. Hashimoto, Y. Shida, N. Yoshikawa, K. Sugimoto, O. Yamakawa, T. Kobayashi, and N. Takahashi, Phys. Rev. Lett. **55**, 2676 (1985).

[2] H. Kitagawa and H. Sagawa, Phys. Lett. B **299**, 1 (1993).

[3] T. Minamisono *et al.*, Phys. Rev. Lett. **69**, 2058 (1992).

[4] W. Schwab *et al.*, Z. Phys. A **350**, 283 (1995).

[5] A. S. Goldhaber, Phys. Lett. **53B**, 306 (1974).

[6] H. Nakada and T. Otsuka, Phys. Rev. C **49**, 886 (1994).

[7] I. Tanihata, T. Kobayashi, O. Yamakawa, S. Shimoura, K. Ekuni, K. Sugimoto, N. Takahashi, T. Shimoda, and H. Sato, Phys. Lett. B **206**, 592 (1988).

[8] R. E. Warner, H. W. Wilschut, W. F. Rulla, and G. N. Felder, Phys. Rev. C **43**, 1313 (1991).

[9] W.-Q. Shen, B. Wang, J. Feng, W.-L. Zhan, Y.-T. Zhu, and E.-P. Feng, Nucl. Phys. **A491**, 130 (1989).

[10] B. M. Sherrill, D. J. Morrissey, J. A. Nolen, Jr., B. Orr, and J. A. Winger, Nucl. Instrum. Methods Phys. Res. Sect. B **70**, 298 (1992).

[11] L. H. Harwood and J. A. Nolen, Jr., Nucl. Instrum. Methods **186**, 435 (1981).

[12] C. F. Williamson, J.-P. Boujot, and J. Picard, Commissariat d'Energie Atomique Report No. R3042, Saclay, 1966.

[13] J. F. Ziegler, *The Stopping and Ranges of Particles in Matter* (Pergamon, New York, 1977), Vol. 4.

[14] S. Kox *et al.*, Phys. Rev. C **35**, 1678 (1987).

[15] G. F. Bertsch, B. A. Brown, and H. Sagawa, Phys. Rev. C **39**, 1154 (1989).

[16] R. E. Warner and G. N. Felder, Phys. Rev. C **42**, 2252 (1990).

[17] C. W. de Jager, H. de Vries, and C. de Vries, At. Data Nucl. Data Tables **14**, 479 (1974).

[18] S. K. Charagi and S. K. Gupta, Phys. Rev. C **41**, 1610 (1990).

[19] A. Muthukrishnan, Senior Honors Thesis, Oberlin College, 1995 (unpublished).

[20] G. Baur, C. A. Bertulani and H. Rebel, Nucl. Phys. **A458**, 188 (1986).

[21] R. W. Kavanagh, *Cosmology, Fusion, and Other Matters* (Colorado Associated University Press, Boulder, Co, 1972), p. 169.

[22] J. S. Levinger and H. A. Bethe, Phys. Rev. **78**, 115 (1950).

[23] I. Tanihata *et al.*, Phys. Lett. B **287**, 307 (1992).

[24] J. H. Kelley *et al.* (unpublished).
[25] T. Motobayashi *et al.*, Phys. Rev. Lett. **73**, 2680 (1994).
[26] D. A. Roberts, F. D. Becchetti, J. A. Brown, J. Jänecke, K. Pham, T. W. O'Donnell, R. E. Warner, R. M. Ronningen, and H. W. Wilschut, in Proceedings of International Symposium on Physics of Unstable Nuceli, Niiigata, Japan, 1994.
[27] I. Pecina *et al.*, Phys. Rev. C **52**, 191 (1995).
[28] R. E. Warner, C. L. Carpenter, J. M. Fetter, W. F. Waite, H. W. Wilschut, and J. M. Hoogduin, Phys. Rev. C **48**, 245 (1993).